Neuro-Oncology
26(5), 872–888, 2024 | https://doi.org/10.1093/neuonc/noad264 | Advance Access date 30 December 2023

Hypoxia-induced galectin-8 maintains stemness in glioma stem cells via autophagy regulation

Dan Liu†, Hongtao Zhu†, Lidong Cheng, Ran Li, Xiaoyu Ma, Jing Wang, Junwen Wang, Suojun Zhang, Yingjie Li, Kai Shu, Xingjiang Yu, and Chuanzhou Li

All author affiliations are listed at the end of the article

†These authors contributed equally.

Corresponding Authors: Kai Shu, Department of Neurosurgery, Tongji Hospital, Tongji Medical College, Huazhong University of Science and Technology, No. 1095 Jiefang Avenue, Wuhan 430030, China (kshu@tjh.tjmu.edu.cn); Xingjiang Yu, Department of Histology and Embryology, School of Basic Medicine, Tongji Medical College, Huazhong University of Science and Technology, No. 13 Hangkong Road, Wuhan 430030, China (yuxingjiang@hust.edu.cn); Department of Medical Genetics, School of Basic Medicine, Tongji Medical College, Huazhong University of Science and Technology, Chuanzhou Li, No. 13 Hangkong Road, Wuhan 430030, China (chuanzhouli@hust.edu.cn).

Abstract

Background. Glioma stem cells (GSCs) are the root cause of relapse and treatment resistance in glioblastoma (GBM). In GSCs, hypoxia in the microenvironment is known to facilitate the maintenance of stem cells, and evolutionally conserved autophagy regulates cell homeostasis to control cell population. The precise involvement of autophagy regulation in hypoxic conditions in maintaining the stemness of GSCs remains unclear.

Methods. The association of autophagy regulation and hypoxia was first assessed by in silico analysis and validation in vitro. Glioma databases and clinical specimens were used to determine galectin-8 (Gal-8) expression in GSCs and human GBMs, and the regulation and function of Gal-8 in stemness maintenance were evaluated by genetic manipulation in vitro and in vivo. How autophagy was stimulated by Gal-8 under hypoxia was systematically investigated.

Results. Hypoxia enhances autophagy in GSCs to facilitate self-renewal, and Gal-8 in the galectin family is specifically involved and expressed in GSCs within the hypoxic niche. Gal-8 is highly expressed in GBM and predicts poor survival in patients. Suppression of Gal-8 prevents tumor growth and prolongs survival in mouse models of GBM. Gal-8 binds to the Ragulator-Rag complex at the lysosome membrane and inactivates mTORC1, leading to the nuclear translocation of downstream TFEB and initiation of autophagic lysosomal biogenesis. Consequently, the survival and proliferative activity of GSCs are maintained.

Conclusions. Our findings reveal a novel Gal-8-mTOR-TFEB axis induced by hypoxia in the maintenance of GSC stemness via autophagy reinforcement, highlighting Gal-8 as a candidate for GSCs-targeted GBM therapy.

Key Points

- Hypoxia-enhanced autophagy contributes to stemness maintenance in GSCs.
- Gal-8 is preferentially induced in GSCs under hypoxia and predicts poor prognosis for glioma patients.
- Gal-8 promotes autophagy and maintains stemness in GSCs via the mTOR-TFEB axis.

Graphical Abstract

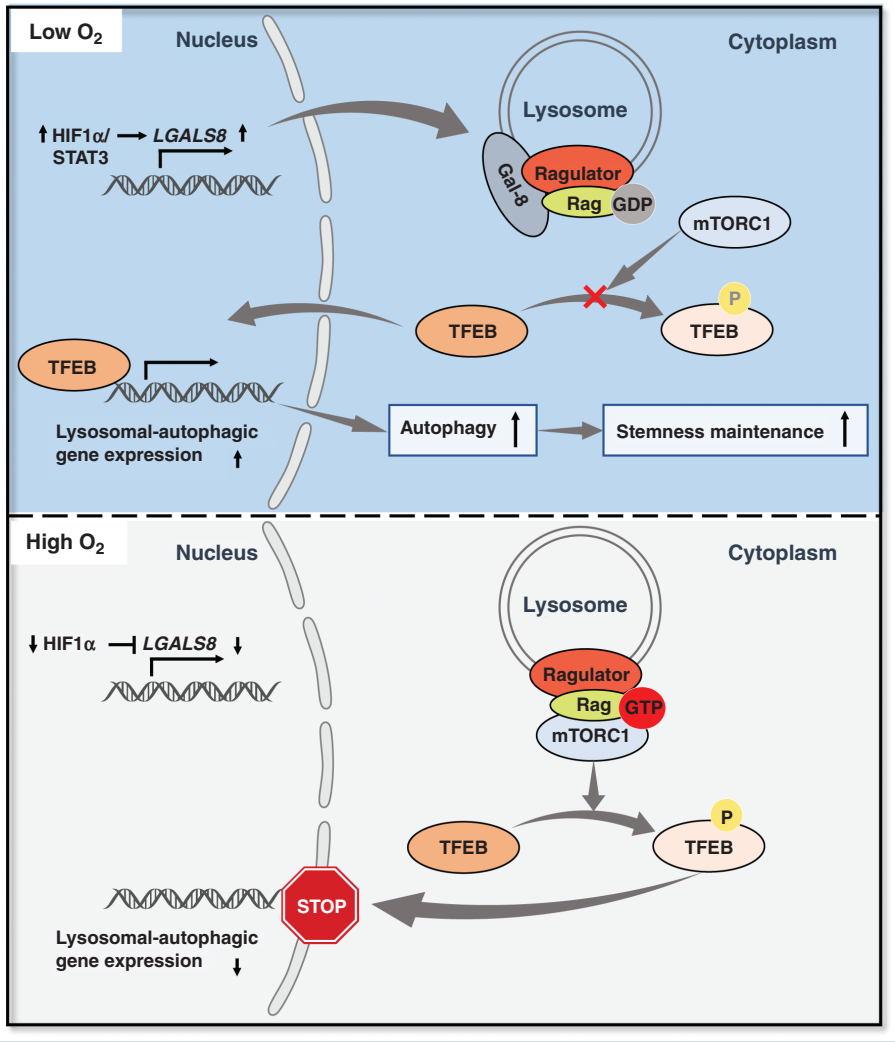

Importance of the Study

Hypoxic niches are a prevalent characterization of the GBM microenvironment and play fundamental roles in GBM malignancy. In this study, we demonstrate that hypoxia, by inducing Gal-8, enhances autophagy to facilitate self-renewal in GSCs. Mechanistically, recruitment of Gal-8 to the Ragulator-Rag complex inhibits mTOR activity, followed by nuclear translocation of TFEB and autophagy-related lysosomal biogenesis, thereby promoting proliferation and self-renewal in GSCs.

Glioblastoma (GBM) is the most common and lethal primary malignant brain tumor in adults, which exhibits rapid proliferation, extensive infiltration, and resistance to radiotherapy and chemotherapy.[1] Standard treatment for GBM is surgical resection followed by radiotherapy and chemotherapy, however, even under maximal medical therapy, the prognosis of GBM patients remains unsatisfactory, with a median survival of 14–16 months and postoperative recurrence inevitably occurring in the majority of patients.[2] Accumulating evidence indicates that the recurrence and treatment resistance of GBM are attributable to glioma stem cells (GSCs), which account for approximately 1%–10% of all cells in the tumor.[3] GSCs exhibit characteristics of tumor initiation, self-renewal, and sustained proliferation, that are widely involved in tumor proliferation, invasion, immunosuppression, metabolic reprogramming, and neovascularization.[4] Therefore, the exploration of novel mechanisms that drive the self-renewal of GSCs may offer valuable insights into GSCs-targeted therapy for GBM.

The hypoxic microenvironment serves as one of the most important factors that determine stemness maintenance of GSCs.[5] Activation of transcription factors such as HIF1α under hypoxia mediates tumor growth, invasion, proneural-mesenchymal transition (PMT), immunosuppression, and treatment resistance through the transcriptional regulation of downstream target genes.[6–9] Hypoxia supports GSC stemness that is characterized by the expression of stem cell markers such as CD133, regulation of tumor invasion, epigenetic modifications, metabolic reprogramming, and interactions with immune cells.[5]Therefore, GSCs tend to be more abundant in hypoxic niches of GBM tumors, and the extent of hypoxia usually correlates with poor prognosis of GBM patients.[10,11]

Autophagy (often referred to as macroautophagy) is an evolutionarily conserved biological process in which cells recycle cytoplasmic components such as protein complexes and dysfunctional organelles into autophagosomes followed by lysosomal degradation to maintain cellular homeostasis.[12] Multiple studies suggest that the autophagic process is dysfunctional in a variety of cancer stem cells (CSCs) and autophagy plays a vital role in maintaining the stemness of CSCs, suggesting that autophagy in CSCs could be a potential target for cancer therapy.[13,14] In GBM, autophagy is associated with multiple processes including PMT, treatment resistance, and immunosuppression.[15,16] In GSCs, enhanced autophagy presented by ATG4B phosphorylation and ATG9B activation promotes stemness maintenance,[17,18] and there are also studies showing that activation of autophagy inhibits self-renewal of GSCs and hinders tumor growth.[19] However, most evidence on autophagy and stemness maintenance of GSCs was concluded under normoxic conditions, and how hypoxia regulates autophagy and stemness maintenance in GSCs is largely elusive.

In the current study, we identified that galectin-8 (Gal-8), as a mediator of hypoxia-induced autophagy and the self-renewal of GSCs, bridges 2 key events, autophagy and stemness maintenance, in GSCs under hypoxia. In brief, Gal-8 predicts poor prognosis for glioma patients and is preferentially induced in GSCs by hypoxia. The reduction of Gal-8 expression disrupts autophagy and suppresses the proliferation and self-renewal of GSCs both in vitro and in GBM-bearing mice. Hypoxia-induced Gal-8 binds to the mTOR complex and initiates the downstream TFEB-regulated activation of autophagolysosomal genes, ultimately sustaining GSCs. Moreover, Gal-8-induced autophagy is validated by pharmacological and genetic modulation of mTOR-TFEB signaling. Taken together, our findings uncover a novel hypoxia-induced Gal-8-mTOR-TFEB axis that links the regulation of autophagy and self-renewal of GSCs within the hypoxic niches.

Materials and Methods

Cell Culture

GBM patient-derived GSCs (T3359, T3691, T4121, and D456) were gifted from Dr. Shideng Bao and Dr. Jeremy Rich. GSCs were cultured in a serum-free system containing Neurobasal A basal medium supplemented with B-27 Supplement Minus Vitamin A, L-glutamine, sodium pyruvate, 20 ng/ml recombinant epidermal growth factor, and 20 ng/ml basic fibroblast growth factor (bFGF). For differentiation, GSCs were digested into single cells by accutase cell detachment solution and seeded in a differentiation medium (DMEM formulated with high glucose 4.5 g/l and supplemented with 10% FBS). Differentiation lasted for 2 weeks and the non-stem tumor cells (NSTCs) were collected in downstream assays. The HEK293T cells were cultured in DMEM medium (high glucose) with 10% FBS and incubated at 37 °C (5% CO_2, 1% O_2) in a multi-gas O_2/CO_2 incubator (ESCO) for hypoxia treatment and 37 °C (5% CO_2) for conventional culture.

Mouse Xenograft Studies

Four-week-old BALB/c nude mice were purchased from the Beijing HFK Bioscience Co. Ltd. Mice were maintained in the pathogen-free barrier animal facility at the Experimental Animal Center of Tongji Medical College, Huazhong University of Science and Technology. For intracranial tumorigenesis, 2×10^4 GSCs transduced with shLGALS8 or shNT were injected into the right frontal lobes of mice. Each group contains 10 mice (5 male and 5 female). When the first neurological signs appeared in the shNT group, we randomly selected a mouse from the shLGALS8 group on the same day to compare the tumor growth. When mice manifest neurological signs, brain tissues are removed after euthanasia. Tissues were fixed with 4% paraformaldehyde (PFA) and embedded in optimal cutting temperature (OCT) compound for frozen sectioning at 10-μm thickness. All animal procedures were performed following the Guide for the Care and Use of Laboratory Animals and approved by the University Animal Welfare Committee, Tongji Medical College, Huazhong University of Science and Technology.

GBM Patient Samples

The use of samples from GBM patients was approved by the Medical Ethics Committee of Tongji Hospital. Fresh GBM patient samples were obtained from the Department of Neurosurgery of Tongji Hospital and were embedded in OCT. Ten micrometer slices were used for immunofluorescence staining. The 91 tissues glioma tissue microarray we established previously[20] was used for immunohistochemistry.

DNA Constructs, Lentivirus Package, and Lentiviral Transduction

The shRNAs targeting human Gal-8, HIF1α, HIF2α, and STAT3 were cloned into pLKO.1 vector for gene knockdown. The coding sequence (CDS) of human Gal-8 was cloned into a pHAGE vector with a FLAG tag and the CDS of human TFEB fused with GFP was cloned into a pLVX vector for overexpression. The sequences of shRNAs used in this study are:

shRNA #355 targeting human *LGALS8*: GCAAAGTG AATATTCACTCAA
shRNA #357 targeting human *LGALS8*: GCTGGAAA TTAATGGAGACAT

shRNA #3808 targeting human *HIF1A*: CCGCTGGAGAC ACAATCATAT
shRNA #3809 targeting human *HIF1A*: CCAGTTATGATT GTGAAGTTA
shRNA #3805 targeting human *HIF2A*: GCGCAAATGTAC CCAATGATA
shRNA #3806 targeting human *HIF2A*: CAGTACCCAGAC GGATTTCAA
shRNA #842 targeting human *STAT3*: GCACAATCTACG AAGAATCAA
shRNA #843 targeting human *STAT3*: GCAAAGAAT CACATGCCACTT
shRNA #474 targeting human *ATG5*: CCTTTCATTCA GAAGCTGTTT
shRNA #395 targeting human *ATG5*: AGATTGAAGGAT CAACTATTT
shRNA #586 targeting human *ATG7*: GCTTTGGGATTTG ACACATTT
shRNA #587 targeting human *ATG7*: CCCAGCTATT GGAACACTGTA

For the lentivirus package, target plasmids were transfected into HEK293T cells together with psPAX2 and pMD2.G using polyethylenimine (PEI) (Yeasen). Twelve hours after transfection, the medium was replaced with a complete GSCs neurobasal A medium. After further incubation for 72 h, the supernatant was collected and filtered by a 0.45-μm filter. For lentiviral transduction of GSCs, the filtered lentiviral supernatant was mixed with fresh GSCs complete neurobasal A medium (1:1) supplemented with polybrene (8 mg/ml, Yeasen) for infection. Transduced cells were selected by 1 μg/ml puromycin (Thermo) for 48 h.

EdU Cell Proliferation Assay

The Cell-Light EdU Apollo643 In Vitro Kit (RIBOBIO, #C10310-2) was applied to detect the proliferative activity of cells according to the manufacturer's instructions. In brief, the EdU solution was incorporated into the GSCs medium and incubated under hypoxia for 2 h. After fixation, washing, staining of EdU, and counterstaining nucleus with Hoechst, the tumor spheres were smeared onto a microscope slide and then imaged by a NIB900-FL fluorescence microscope (Nexcope). The ratio of EdU-positive cells to total nuclei was obtained to indicate proliferation.

Cell Viability Assay

For cell viability assays, GSCs were seeded into 96-well plates at a density of 1500 cells/well. Cell viability was measured by an EnSpire multimode plate reader (PerkinElmer) at days 0, 1, 3, and 5 using a Cell Titer-Glo Luminescent Cell Viability Assay kit (Promega). At least 3 repeats were performed and all data were normalized to day 0 and presented as mean ± SEM.

Sphereformation Assay

For sphereformation assay, GSCs of each group were seeded into 24-well plates at a density of 2000 cells/well with 3 replicates in each group. The number of tumor spheres in each well was recorded and analyzed after 5 days.

In Vitro Limiting Dilution Assay

For the in vitro limiting dilution assay, a gradient number of GSCs (1, 10, 20, 30, 40, and 50 cells) were seeded into a 96-well plate, and 8 replicates were conducted for each gradient. After 7 days, the formation and number of tumor spheres in each well were recorded. The self-renewal capacity of GSCs in each group was analyzed by the Extreme Limiting Dilution Analysis.[21]

Bioinformatics analysis

The microarray/RNA-seq mRNA expression data, molecular pathological status (*IDH1* and 1p19q), and survival data of glioma patients of TCGA database, CGGA database, Rembrandt database, and Gravendeel database were downloaded from GlioVis (http://gliovis.bioinfo.cnio.es).[22] The Gene set enrichment analysis (GSEA) was performed by GSEA4.1.0 version software and the enriched pathways were sorted by the normalized enrichment score (NES) and the false discovery rate (FDR). R package "EdgeR" was used to determine differential genes (DEGs) between GBM samples of the TCGA-GBM database and the normal cortex of the GTEx database. The ssGSEA algorithm based on the R package "GSVA" was used to calculate ssGSEA score levels. The weighted correlation network analysis was performed by the R package "WGCNA."

Statistical Analysis

Statistical analysis was performed using GraphPad Prism 7.0 software. Differences were determined by 2-tailed unpaired Student's *t*-test between 2 groups, and 2-way analysis of variance (ANOVA) for multiple comparisons. All experiments were repeated more than 3 times and the data used in this study are presented as the mean ± SEM unless otherwise specified. $P < .05$ was considered statistically significant.

Results

Hypoxia-Induced Autophagy Promotes GSCs Stemness Maintenance

Since HIF1α is well-known as a key transcription factor activated under hypoxia and is frequently utilized as a marker for hypoxia,[9] to explore the potential regulating impact of hypoxia on autophagy and GSCs, we examined glioma patients in 2 publicly available cancer genome databases, Chinese Glioma Genome Atlas (CGGA), and The Cancer Genome Atlas (TCGA), and we classified the patients into *HIF1A*-high and *HIF1A*-low group based on the transcriptional levels of HIF1α-encoding gene *HIF1A*. Pathway enrichment analysis using the GSEA algorithm showed that apart from "Hypoxia," pathways including "Stemness_up" and 'Autophagy' were also activated in the *HIF1A*-high

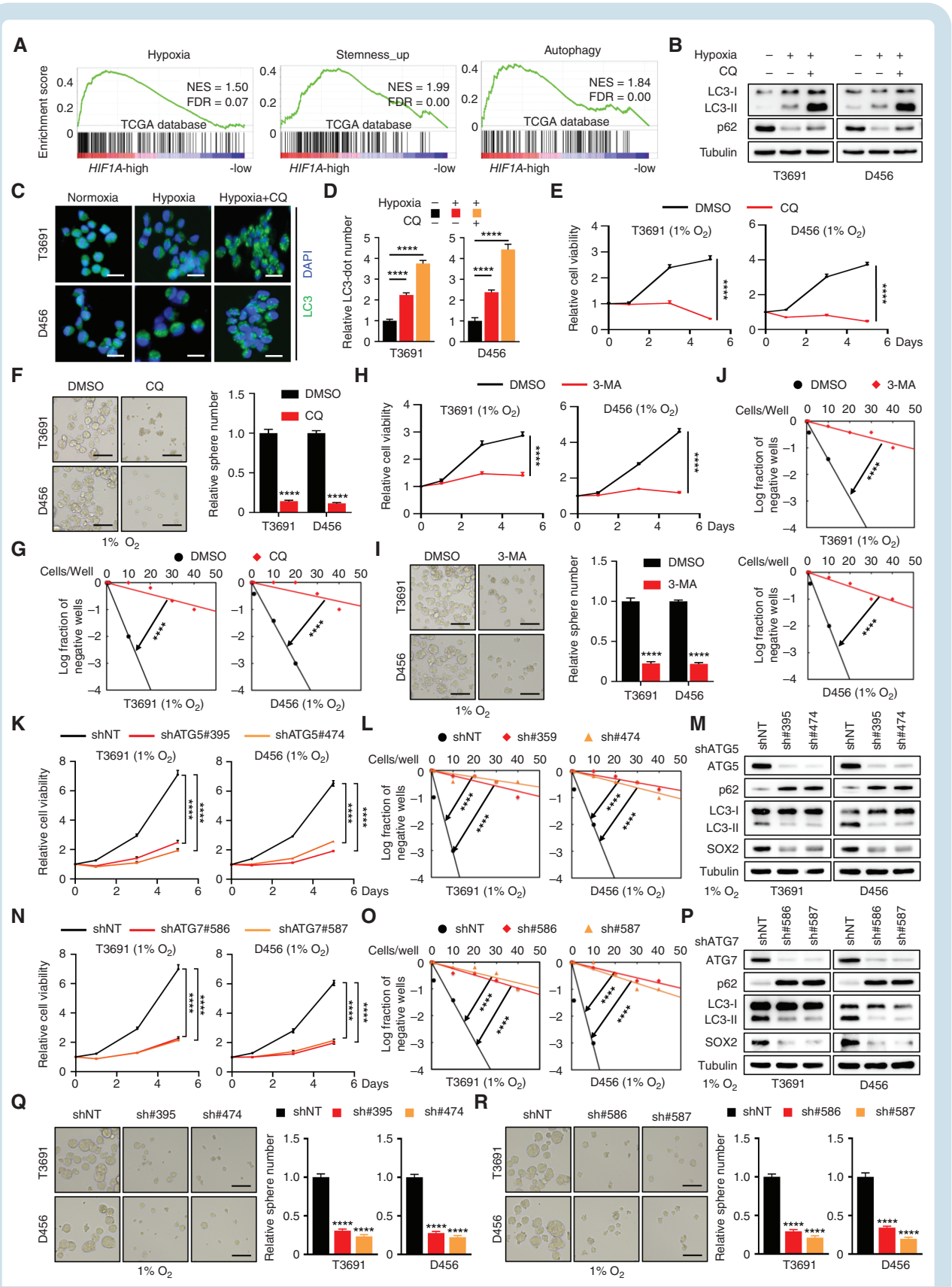

Figure 1. Hypoxia-induced autophagy promotes stemness maintenance in GSCs. (A) GSEA for hypoxia, stemness_up, and autophagy signatures in *HIF1A*-high and *HIF1A*-low patients in the TCGA database. FDR, false discovery rate; NES, normalized enrichment score; (B) Western blot analysis of LC3-I/II and p62 expression in GSCs treated with hypoxia and CQ. (C and D) IF staining of LC3 in GSCs treated with hypoxia and CQ (C).

Quantification of the relative number of LC3-puncta (D). Blue: DAPI-labeled nuclei. Scale bar, 20 μm. (E) Cell viability analysis of GSCs treated with CQ (20 nM) under hypoxia. (F) Sphereformation (left panel) of GSCs treated with DMSO or CQ under hypoxia and quantification of relative sphere number in each group (right panel). Scale bar, 100 μm. (G) In vitro limiting dilution assay of GSCs treated with CQ under hypoxia. (H) Cell viability of GSCs treated with 3-MA (5 mM) under hypoxia. (I) Sphereformation (left panel) of GSCs treated with 3-MA under hypoxia and quantification of relative sphere number in each group (right panel). Scale bar, 100 μm. (J) In vitro limiting dilution assay of GSCs treated with 3-MA under hypoxia. (K) Cell viability analysis of GSCs with ATG5 knockdown under hypoxia. (L) In vitro limiting dilution assay of GSCs with ATG5 knockdown under hypoxia. (M) Western blot analysis of ATG5, LC3-I/II, p62, and stemness marker (SOX2) expression in GSCs with ATG5 knockdown under hypoxia. (N) Cell viability analysis of GSCs with ATG7 knockdown under hypoxia. (O) In vitro limiting dilution assay of GSCs with ATG7 knockdown under hypoxia. (P) Western blot analysis of ATG7, LC3-I/II, p62, and stemness marker (SOX2) expression in GSCs with ATG7 knockdown under hypoxia. (Q) Sphereformation of GSCs with ATG5 knockdown under hypoxia (left panel) and quantification of relative sphere number in each group (right panel). Scale bar, 100 μm. (R) Sphereformation of GSCs with ATG7 knockdown under hypoxia (left panel) and quantification of relative sphere number in each group (right panel). Scale bar, 100 μm. ****$P < .0001$. Data are represented as mean ± SEM.

group compared to the *HIF1A*-low group in 2 databases (Figure 1A, Supplementary Figure 1A–C**)**. This suggests that hypoxia is highly likely to promote GSC stemness and boost autophagy in GBM.

To validate the above in silico analysis, we cultured patient-derived GSCs under hypoxic conditions (1% O_2), and detected expressions of autophagy-related (ATG) genes at both transcriptional and translational levels. As anticipated, in multiple patient-derived GSCs, autophagy was enhanced under hypoxia, as evidenced by upregulated mRNA levels of ATG genes including *BECN1*, *ATG5*, *ATG7*, *ULK1*, *ATG13*, *RB1CC1*, and *ATG101* (Supplementary Figure 1D and E), and the increased and decreased protein level of 2 hallmark ATG proteins, LC3-II and p62, respectively (Supplementary Figure 1F). Moreover, treatment of chloroquine (CQ), an autophagy inhibitor used to intercept the fusion of autophagosome and lysosome, resulted in elevated levels of LC3-II and p62, (Figure 1B, Supplementary Figure 1G), as well as cumulative intracellular LC3-positive puncta (Figure 1C and D**)**, indicating the presence of accumulated autophagosomes in hypoxic GSCs. These findings demonstrate that hypoxia enhances autophagic flux in GSCs.

We and others have reported that hypoxia supports the stem cell characteristics of GSCs.[7,11] To investigate the potential involvement of autophagy, GSCs were challenged with 2 autophagy inhibitors CQ and 3-methyladenine (3-MA) followed by determination of stemness-related phenotypes. Both CQ and 3-MA significantly inhibited the cell viability (Figure 1E and H) and spherefomation of GSCs under hypoxia (Figure 1F and I). The in vitro limiting dilution assay also demonstrated that both inhibitors notably disrupted the survival of GSCs (Figure 1G and J), indicating compromised proliferation and self-renewal of GSCs. Moreover, when autophagy regulators ATG5 and ATG7 were downregulated by lentiviral expression of short hairpin RNAs (shRNAs), both knockdowns resulted in suppressed cell viability (Figure 1K and N) and spherefomation of GSCs under hypoxia (Figure 1Q and R). In vitro limiting dilution assay also indicated that both knockdowns significantly decreased the self-renewal of GSCs (Figure 1L and O). Both knockdown groups showed decreased levels of LC3-II and increased levels of p62, indicative of attenuated autophagy. Consistent with expectations, expression of the stemness marker SOX2 was significantly diminished (Figure 1M and P). Collectively, these findings prompt a regulatory role of autophagy in stemness maintenance of GSCs under hypoxic conditions.

Gal-8 Mediated Hypoxic Induction of Autophagy Maintains GSCs

Since we previously showed that elevated expression of Galectin (Gal, encoded by *LGALS* genes) family members in GBM correlates with hypoxic microenvironment and stemness maintenance of GSCs,[20] and have also reviewed the therapeutic potential of Gal family in autophagy regulation in various tumors,[23] we now wonder if Gal family members directly regulate autophagy and maintain stemness by sensing the hypoxic microenvironment in GSCs.

Gal family comprises evolutionarily conserved glycoconjugated proteins consisting of 16 members involved in embryonic development, immune regulation, cell migration, and autophagy regulation.[23] Given that Gals are also widely implicated in tumor invasion and immunosuppression, they are drawing increasing attention to cancer therapy.[24] As we have reported previously, the expression of 5 Gal family members (Gal-1, Gal-3, Gal-3BP, Gal-8, Gal-9) could indicate poor prognosis for glioma patients in 3 independent databases, TCGA, CGGA, and Rembrandt.[20] The correlations between these 5 Gals and hypoxia markers (*HIF1A*, *VEGFA*, *PGK1*), GSCs markers (*PROM1*, *FUT4*, *CD44*) and autophagy markers (*ATG5*, *ULK1*, *BECN1*) demonstrated highest correlation coefficient of Gal-8 (encoded by *LGALS8* gene). This suggests that Gal-8 is highly likely to mediate autophagy under hypoxia to promote GSC maintenance (Supplementary Figure 2A–D). To unbiasedly validate the involvement of Gal-8 in this process, we utilized ssGSEA algorithm and weighted correlation network analysis (WGCNA) to identify the genes related to hypoxia, stemness, and autophagy concurrently, and 218 genes were retrieved (Supplementary Figure 3A–G). Co-expression analysis further identified the top 30 core nodes within the network and surprisingly revealed that *LGALS8* is of the highest rank (Supplementary Figure 3H).

Gal-8 Correlates With Stemness and Poor Prognosis in Glioma

To investigate the clinical characteristics of Gal-8 in GBM, the mRNA expression of the *LGALS8* gene in glioma patients at various grades in TCGA and CGGA databases was analyzed, and it is shown that Gal-8 expression increases with tumor grade (Figure 2A and B). Moreover, Gal-8 was highly expressed in patients with *IDH1*-WT and

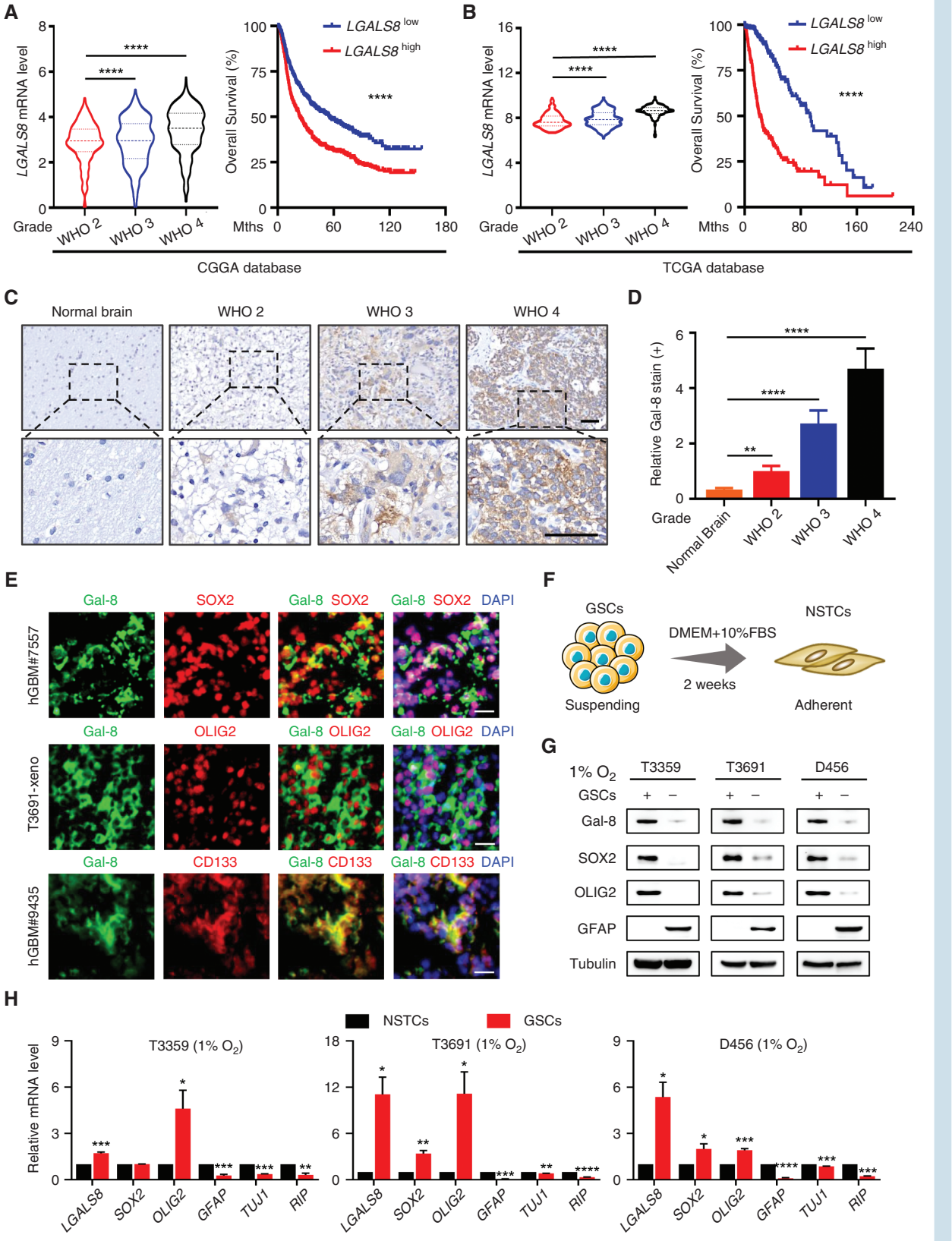

Figure 2. Gal-8 predicts poor prognosis for glioma patients and is preferentially expressed by GSCs. (A) Gal-8 (encoded by *LGALS8* gene) expression in glioma samples with different grades from the CGGA database (left). Kaplan–Meier survival analysis of Gal-8 expression and the overall survival of glioma patients from CGGA database (right). (B) Gal-8 (encoded by *LGALS8* gene) expression in glioma samples with different grades from the TCGA database (left). Kaplan–Meier survival analysis of Gal-8 expression and the overall survival of glioma patients from TCGA

database (right). (C) Representative images of IHC staining of Gal-8 in normal brain and different grades of gliomas within the glioma tissue microarray. Scale bar, 50 μm. (D) The relative positive stain ratios of Gal-8 in each group were quantified by IHCProfile algorithm. (E) Immunofluorescent co-staining of Gal-8 (green) and the markers for GSCs (SOX2, OLIG2, and CD133) (red) in GBM tissues and GSCs-derived xenografts. Blue: DAPI-labeled nuclei. Scale Bar, 25 μm. (F) The schematic illustration of suspending GSCs differentiation to adherent non-stem tumor cells (NSTCs). (G) Western blot analysis of Gal-8, GSC markers (SOX2, OLIG2), and astrocyte/glial marker (GFAP) expression indicative of differentiation in GSCs and matched NSTCs cultured under 24 h of hypoxia. (H) qRT-PCR analysis of *LGALS8* (genes that encode Gal-8), GSC markers (*SOX2*, *OLIG2*), and differentiation markers (*GFAP*, *TUJ1*, *RIP*) expression in GSCs and matched NSTCs cultured under hypoxia for 24 h. $^{**}P < .01$; $^{****}P < .0001$. Data are represented as mean ± SEM.

1p19q Non-Co-deletion (Supplementary Figure 4A and B). A higher expression of Gal-8 correlates with a poorer prognosis as indicated by the survival analysis both in Glioma with all grades and GBM from various databases (Figure 2A and B and Supplementary Figure 4C). In support, further validation by immunohistochemical (IHC) staining of a 91-sample glioma tissue microarray that includes normal brain and glioma tissues at various grades indicates that the protein levels of Gal-8 were higher in glioma tissues and correlated with tumor grade (Figure 2C and D). Next, we evaluated Gal-8 in individual GBM patients and GSCs-derived mouse intracranial xenografts, which showed that Gal-8 co-expresses with CD133, SOX2, and OLIG2 (GSC markers) in GSCs from both origins (Figure 2E, Supplementary Figure 4D–F, Supplementary Figure 4H–I).

We then asked if Gal-8 is uniquely expressed in GSCs and differentiated GSCs into adherent non-stem tumor cells (NSTCs) using fetal bovine serum (FBS) (Figure 2F). As expected, Gal-8 and markers for GSCs (SOX2, OLIG2, and CD133) were preferentially expressed by GSCs, whereas astrocyte marker GFAP was only expressed by NSTCs (Figure 2G, Supplementary Figure 4G). These findings were also confirmed at the transcriptional level (Figure 2H).

Gal-8 is Induced by Hypoxia-Activated STAT3/HIF1α in GSCs

Given that GSC stemness is believed to predict the tumorigenic potential and that hypoxia is conducive to GSC survival, in both tumors of GBM patients and GSCs-derived mouse xenografts, our results demonstrated that Gal-8 was co-localized/co-expressed with CA9/HIF1α (hypoxia markers) in hypoxic regions where GSCs are predominantly present (Figure 3A, Supplementary Figure 5A–D). Moreover, in multiple cultured GSCs, hypoxia treatment stimulated drastic expression of HIF1α and HIF2α, Gal-8 expression, and gene expression of *LGALS8* and other hypoxia markers (*CA9*, *PDK1*, *PGK1*) (Figure 3B, Supplementary Figure 5E). These findings illustrate that Gal-8 induction is highly sensitive and responsive to the hypoxic status in GSCs.

To determine if HIF1α and HIF2α directly regulate Gal-8 expression, we used lentivirus-mediated shRNA to knock down HIF1α and HIF2α expression in GSCs. When HIF1α expression was suppressed, hypoxia induction of Gal-8 was abolished at both mRNA and protein levels, while HIF2α expression remained unaltered (Figure 3C and D). In contrast, the knockdown of HIF2α did not affect the mRNA and protein expression of Gal-8 or HIF1α expression in hypoxic GSCs (Figure 3E and F), suggesting that HIF1α rather than HIF2α controls hypoxic induction of Gal-8. Moreover, when Gal-8 expression was depleted under hypoxia, neither HIF1α mRNA nor protein level was affected (Supplementary Figure 5H and I).

We and others have previously indicated the STAT3/HIF1α is co-activated under hypoxia and maintains the self-renewal of GSCs by induction of target gene expression.[7,11] In line with this, mRNA expression of Gal-8 was positively correlated with *HIF1A* and *STAT3* in the CGGA and Gravendeel datasets (Supplementary Figure 5F and G). Notably, the knockdown of STAT3 not only inhibited HIF1α expression but also abolished the expression of Gal-8 transcripts and protein (Figure 3G and H). Collectively, these results confirmed that Gal-8 is another target gene of the STAT3/HIF1α signaling that is activated in GSCs under hypoxia.

Gal-8 is Required for GSC Proliferation and Self-Renewal

To assess if Gal-8 maintains stemness in GSCs, lentivirus expressing 2 distinct shRNAs (shLGALS8#355 and shLGALS8#357) targeting Gal-8 were transduced into GSCs (Supplementary Figure 6A). The knockdown of Gal-8 significantly reduced the cell activity as shown by the cell viability assay in three different GSCs (Figure 4A, Supplementary Figure 6G). Self-renewal of GSCs was also suppressed by Gal-8 knockdown, as demonstrated by the in vitro limiting dilution assay (Figure 4B, Supplementary Figure 6F). A reduced number of tumor spheres were formed after knockdown (Figure 4C and D and Supplementary Figure 6B and D), which was partially attributed to attenuated cell proliferation suggested by EdU-labeled replicating cells (Figure 4E and F and Supplementary Figure 6C and E). We then evaluated the differentiation status of Gal-8 depleted cells and found reduced expression of stemness markers (SOX2, OLIG2), as well as enhanced differentiation and apoptosis in these cells (Figure 4G and H and Supplementary Figure 6H–M). Furthermore, Gal-8-overexpressing lentivirus (Supplementary Figure 7A) augmented the proliferation and sphereformation in GSCs (Supplementary Figure 7B–D). Moreover, since temozolomide is the first-line chemotherapeutic agent for GBM treatment and GSCs are the root cause of temozolomide resistance,[25] to investigate the treatment-related implications of Gal-8, we treated GSCs with temozolomide in combination with Gal-8 knockdown or overexpression. We found that temozolomide-induced cytotoxicity, apoptosis, and suppression of proliferation were aggravated by Gal-8 knockdown, whereas Gal-8 overexpression reduced temozolomide-stimulated apoptosis (Supplementary Figure 8A–F).

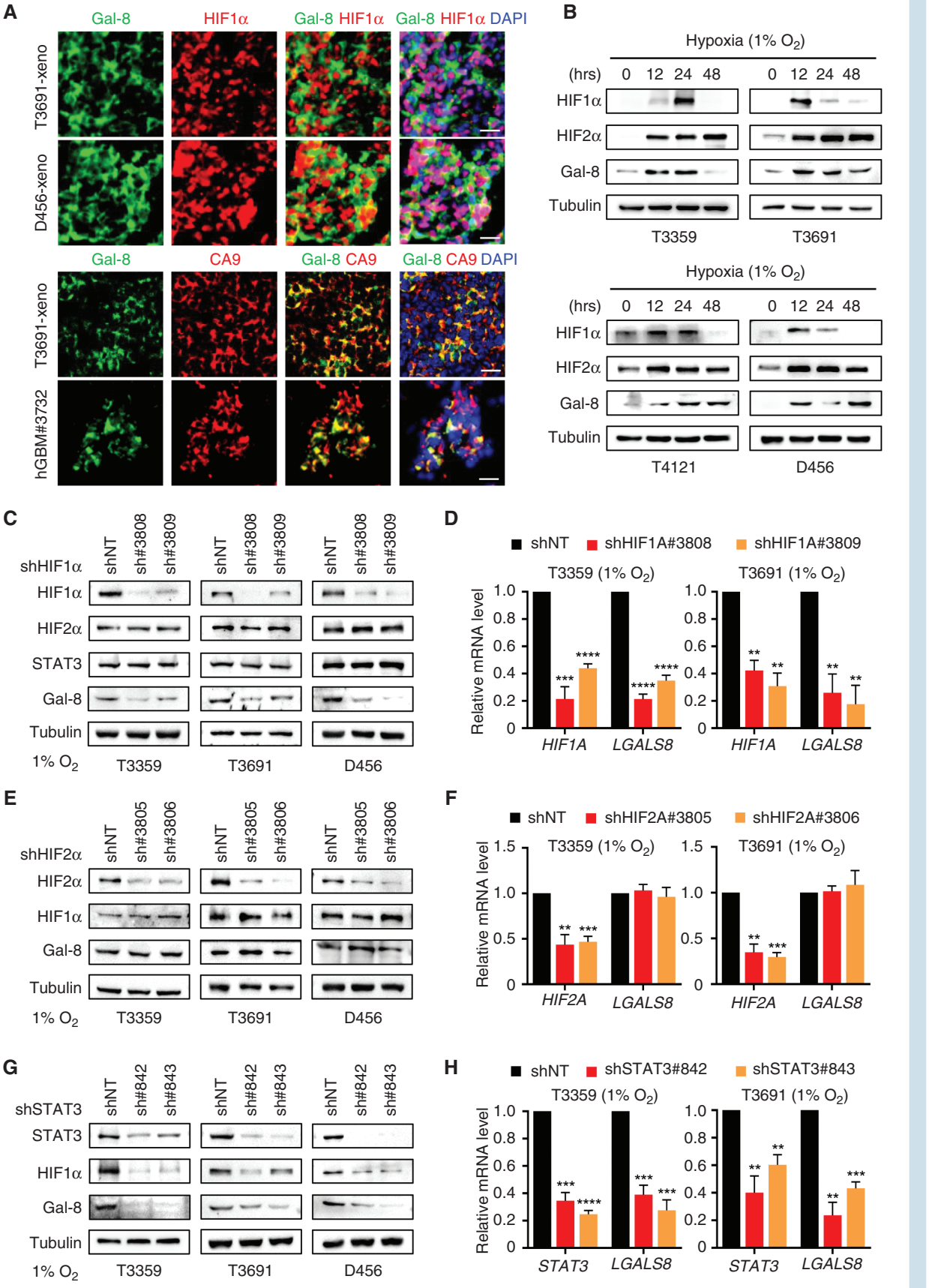

Figure 3. Gal-8 is induced by hypoxia-activated STAT3/HIF1α in GSCs. (A) Immunofluorescent co-staining of Gal-8 (green) and the markers for hypoxia (HIF1α and CA9) (red) in patient GBM tissues and GSCs-derived xenografts. Blue: DAPI-labeled nuclei. Scale Bar, 25 μm. (B) Western blot

analysis of Gal-8, HIF1α, and HIF2α expression in GSCs cultured under normoxia or hypoxia for the indicated period. (C) Western blot analysis of Gal-8, HIF1α, HIF2α, and STAT3 expression in GSCs transduced with 2 distinct shRNAs targeting HIF1α through lentiviral infection. GSCs were cultured under hypoxia for 24 h. (D) qRT-PCR analysis of *LGALS8* (the gene that encodes Gal-8) and *HIF1A* expression in GSCs transduced with shRNAs targeting *HIF1A* through lentiviral infection. GSCs were cultured under hypoxia for 24 h. (E) Western blot analysis of Gal-8, HIF1α, and HIF2α expression in GSCs transduced with 2 distinct shRNAs targeting HIF2α through lentiviral infection. GSCs were cultured under hypoxia for 24 h. (F) qRT-PCR analysis of *LGALS8* (genes that encode Gal-8) and *HIF2A* expression in GSCs transduced with lentivirus expressing shRNAs targeting *HIF2A*. GSCs were cultured under hypoxia for 24 h. (G) Western blot analysis of Gal-8, HIF1α, and STAT3 expression in GSCs transduced with shRNAs targeting STAT3 through lentiviral infection. GSCs were cultured under hypoxia for 24 h. (H) qRT-PCR analysis of *LGALS8* (the gene that encodes Gal-8) and *STAT3* expression in GSCs transduced with two distinct shRNAs targeting *STAT3* through lentiviral infection. GSCs were cultured under hypoxia for 24 h. $^{*}P < 0.05$; $^{**}P < 0.01$; $^{***}P < 0.001$; $^{****}P < 0.0001$. Data are represented as mean ± SEM.

Collectively, these data highlight the role of Gal-8 as a crucial regulator for GSC proliferation and self-renewal, as well as its clinical value in tackling chemoresistance in GBM.

Next, we transduced GSCs with lentiviral expression of shLGALS8 or shNT and intracranially injected cells into the brains of immunocompromised nude mice. H&E staining of brain slices indicated markedly diminished tumor growth with Gal-8 knockdown (Figure 4J). Consistent with expectations, mice transplanted with shLGALS8-expressing GSCs exhibited a longer survival time than mice in the shNT group (Figure 4I). Xenografts from the shLGALS8 group showed suppressed proliferation indicated by Ki67, and augmented apoptosis, as suggested by more TUNEL-positive cells and cleaved caspase3-positive cells compared to the control (Figure 4K, L; Supplementary Figure 9A). Moreover, the knockdown group also exhibited much lower expression of GSCs markers (SOX2, CD133, CD15) and more intense GFAP staining (Figure 4K and L; Supplementary Figure 9B). This indicates that disrupting Gal-8 leads to a decrease in the proportion of GSCs in tumor cells, through the regulation of proliferation, apoptosis, and self-renewal properties in GSCs.

Gal-8 Binds to the Ragulator-Rag Complex to Potentiate Autophagy Through mTOR-TFEB Axis

We used the GSEA algorithm to unbiasedly analyze the pathway enrichment in *LGALS8*-high and *LGALS8*-low groups of glioma patients in the CGGA and Rembrandt databases and revealed that the "Autophagy" pathway was virtually activated in the *LGALS8*-high group other than the *LGALS8*-low group in both datasets (Supplementary Figure 10A and B). RNA-seq analysis of GSCs expressing shLGALS8 or shNT revealed a notably elevated mRNA expression of ATG genes in the shLGALS8 group (Supplementary Figure 10C). In support of the in silico finding, qRT-PCR, western blotting, and IF were performed for validation of autophagy. The mRNA levels of ATG genes (*BECN1*, *ATG5*, *ATG7*, *ULK1*, *ATG13*, *RB1CC1*, and *ATG101*) were significantly downregulated following Gal-8 knockdown under hypoxia, concomitant with decreased LC3-II and increased p62 indicative of attenuated autophagy (Supplementary Figure 10D and E; Figure 5A). The LC3-dot numbers were markedly lower in the shLGALS8 group both in GSCs and xenografts (Figure 5B and C). Additionally, overexpression of Gal-8 under hypoxic conditions completely reversed the changes of LC3-II and p62 expression induced by the depletion of Gal-8 (Figure 5D). These findings strongly suggest that Gal-8 could directly potentiate autophagy in GSCs.

To identify potential autophagy-related pathways regulated by Gal-8, we performed GSEA analysis in glioma patients and found that higher Gal-8 expression correlates with inhibited mTOR-signaling and elevated expression of transcription factor EB (TFEB) target genes (Figure 5E). The regulation of autophagy by mTOR-TFEB signaling has been well established.[26] In brief, the activated form of mTOR phosphorylates TFEB, preventing its entry into the nucleus; when mTOR is inhibited under autophagic stimuli, nuclear translocation of non-phosphorylated TFEB promotes lysosomal biogenesis and the transcription of downstream targets such as ATG genes, thereby further activating autophagy.[26] Nonetheless, in the hypoxic microenvironment of GBM, how the mTOR-TFEB axis is modulated is still underexplored. As anticipated, a hypoxic condition in GSCs induced decreased phosphorylation of mTOR and TFEB (Figure 5F), and increased presence of nuclear TFEB followed by transcriptional activation of TFEB target genes (*WIP1*, *ATG9B*, *LAMP1*) (Supplementary Figure 11A–C). The impact of Gal-8 on the mTOR-TFEB axis was then investigated and the results showed that Gal-8 knockdown upregulated the protein levels of p-mTOR and p-TFEB (Figure 5G), which resulted in decreased nuclear TFEB and transcriptional inhibition of TFEB target genes in GSCs and xenografts (Figure 5H–J; Supplementary Figure 11D–E). Furthermore, the overexpression of Gal-8 leads to the inhibition of mTOR, increased nuclear translocation of TFEB, and activated transcription of TFEB target genes (Figure 5K; Supplementary Figure 11F–H).

We next asked how Gal-8 modulates mTOR activity. The Ragulator-Rag complex located on the lysosomal membrane regulates mTOR activity by recruiting mTORC1 to the lysosomal membrane via active Rags (GTP state).[27] Gal-8 has been reported to bind to the Ragulator-Rag complex, which inhibits Rag activity and dissociates the mTORC1 complex from the lysosomal membrane, thereby deactivating mTOR.[28] Co-immunoprecipitation (co-IP) assay with the extracts of FLAG-Gal-8 overexpressing GSCs under hypoxia indicated that Gal-8 physically associates with RagA/B/C/D and lamtor1 (Figure 5L). Taken together, these results illustrate that hypoxic induction of Gal-8 binds to the Ragulator-Rag complex and inhibits mTOR, which sequentially promotes the nuclear translocation of TFEB and downstream autophagic regulation.

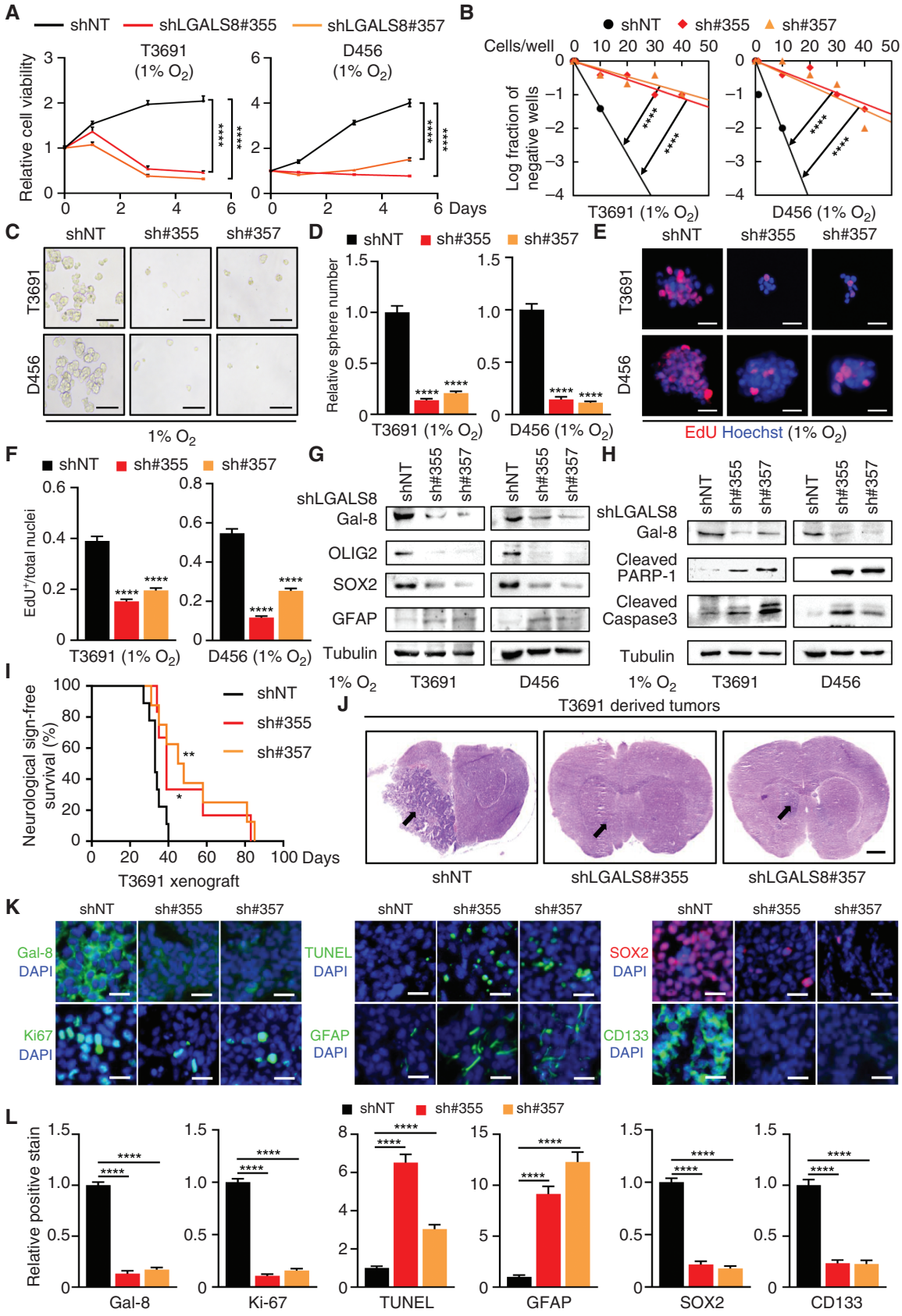

Figure 4. Gal-8 is required for GSC proliferation and self-renewal. (A) Cell viability analysis of GSCs with Gal-8 knockdown under hypoxia. (B) In vitro limiting dilution assay of GSCs with Gal-8 knockdown under hypoxia. (C and D) Sphereformation of GSCs with Gal-8 knockdown under hypoxia (C) and quantification of relative sphere number in each group (D). Scale bar, 100 μm. (E and F) EdU proliferation assay (F) of GSCs with Gal-8

knockdown under hypoxia and the quantification of EdU + cells in each group (G). Blue: Hoechst-labeled nuclei. Scale bar, 25 μm. (G) Western blot analysis of Gal-8, GSC markers (SOX2, OLIG2), and differentiation marker (GFAP) expression in GSCs with Gal-8 knockdown under hypoxia. (H) Western blot analysis of Gal-8 and apoptosis markers (cleaved PARP-1 and cleaved caspase3) expression in GSCs with Gal-8 knockdown under hypoxia. (I) Kaplan–Meier survival curve of mice injected with GSCs expressing shNT or shLGALS8 (n = 10 per group). (J) H&E staining of mouse brains in the shNT and shLGALS8 group 25 days after transplantation. The arrows indicate tumors. Scale Bar, 1000 μm. (K) Immunofluorescent staining of Gal-8, proliferation marker (Ki67), GSC markers (SOX2, CD133), differentiation marker (GFAP), and TUNEL staining in xenografts derived from GSCs with depletion of Gal-8 by shLGALS8. Blue: DAPI-labeled nuclei. Scale Bar, 50 μm. (L) The quantification of relative staining in each group of K. *P < .05; **P < .01; ****P < .0001. Data are represented as mean ± SEM.

Modulation of mTOR/TFEB Axis Mitigates the Reduction in Autophagy Induced by Gal-8 Depletion

We then investigated whether regulation of the mTOR/TFEB axis is sufficient to govern the autophagy-mediated self-renewal of GSCs, independent of Gal-8. Various concentrations of Rapamycin inhibited the activity of mTOR and its canonical substrate S6K, as well as TFEB (Supplementary Figure 12A), and not surprisingly, notably increased nuclearTFEB was observed following Rapamycin treatment (Supplementary Figure 12B–D). To minimize the effect of Gal-8, we first depleted Gal-8 in hypoxic GSCs and then administered Rapamycin treatment. The knockdown of Gal-8 triggered activation of mTOR-TFEB and attenuated autophagy, as indicated by less LC3-II and accumulated p62, all of which were reversed by Rapamycin treatment (Figure 6A). Consequently, augmented nuclear transport of TFEB (Figure 6B) and enhanced transcription of its target genes were observed (Figure 6C). Moreover, in hypoxic GSCs after Gal-8 depletion, reduced autophagy was reversed when TFEB was ectopically overexpressed (Figure 6D), meanwhile, cell proliferation and self-renewal of GSCs were also restored (Figure 6E–G). Together, these findings demonstrated that mTOR inhibition or TFEB overexpression can rescue the autophagy reduction caused by the suppression of Gal-8, thereby providing additional evidence for the regulatory function of the hypoxia-induced Gal-8-mTOR-TFEB axis in autophagy and self-renewal of GSCs.

Discussion

Gal-8, a "tandem-repeat"-type galectin, is involved in the development, angiogenesis, cell differentiation, adhesion, and protective autophagy under physiological conditions.[29,30] Additionally, it is widely implicated in malignant progression and is considered an indicator of poor prognosis in various types of tumors including cervical cancer, breast cancer, prostate cancer, clear cell renal cell carcinoma, etc.[31–37] We and others have reported that Gal-8 promotes the proliferation and invasion of GBM cell lines in vitro and its high expression suggests poor prognosis in GBM patients.[20,38] However, notwithstanding the bioinformatics analysis and in vitro phenotypic experiments conducted in conventional cell lines in Gal-8-related studies, the expression characteristics of Gal-8 in GBM tumors and the detailed mechanisms of how it facilitates GBM progression remain largely unknown. Herein we have identified that Gal-8 is preferentially expressed in GSCs located in the hypoxic niches of GBM, and is transcriptionally induced by the STAT3/HIF1α signaling under hypoxia. Downregulation of Gal-8 markedly reduced GSC proliferation and self-renewal both in vitro and in vivo. Mechanistically, this study demonstrated that the binding of Gal-8 to the Ragulator-Rag complex inhibits mTOR and promotes TFEB nuclear transport, which enhances autophagy and finally facilitates the proliferation and self-renewal of GSCs. Our study offers a comprehensive description of the expression, function, and regulatory mechanism of Gal-8 in GSCs and GBM progression, underscoring the therapeutic potential of Gal-8 in treatments targeting GSCs in GBM.

Hypoxia is a hallmark characteristic associated with malignant phenotypes and predicts poor prognosis for patients with various cancers, including GBM.[39] Hypoxic niches are prevalent in GBM tumors and histologically manifest as "pseudopalisading" necrosis.[40] Since the hypoxic microenvironment and the HIF pathways play vital roles in angiogenesis, invasion, and treatment resistance of GBM, they are considered promising targets for GBM therapy. Notably, GSCs, a small portion of tumor cells with stemness properties, are particularly enriched within the GBM hypoxic niches and exhibit a strong capacity for tumor-initiating and resistance to chemoradiotherapy. Hence, understanding how GSCs maintain their stem cell programs under hypoxia would provide valuable insights into GSC-targeted therapy. In this study, a novel hypoxia-induced protein, Gal-8, has been identified to promote the self-renewal of GSCs in vitro and to accelerate intracranial tumor growth derived from GSCs in immunocompromised nude mice, by enhancing mTOR/TFEB-mediated autophagy. Additionally, Gal-8 is preferentially expressed in hypoxic GSCs, and our preliminary data also indicate the benefits of Gal-8 inhibition in overcoming temozolomide-induced chemoresistance, suggesting that targeting Gal-8 may precisely trace GSCs and improve the prognosis of GBM.

Numerous studies have shown that autophagy is dysfunctional in various types of tumors.[41] Modulators of autophagy, such as both autophagy inhibitors and autophagy inducers, have been widely used either alone or in combination with other anti-tumor therapies in clinical trials for cancer therapy.[23] Hydroxychloroquine (HCQ), an autophagy inhibitor, has been employed to treat newly diagnosed GBM in combination with radiotherapy and adjuvant temozolomide in a phase I/II clinical trial. Nevertheless, compared to chemoradiotherapy alone, no significant prolongation of overall survival was recorded after additional treatment of HCQ, despite the inhibition of autophagy by HCQ.[42] One reason for this failure could be attributed to the

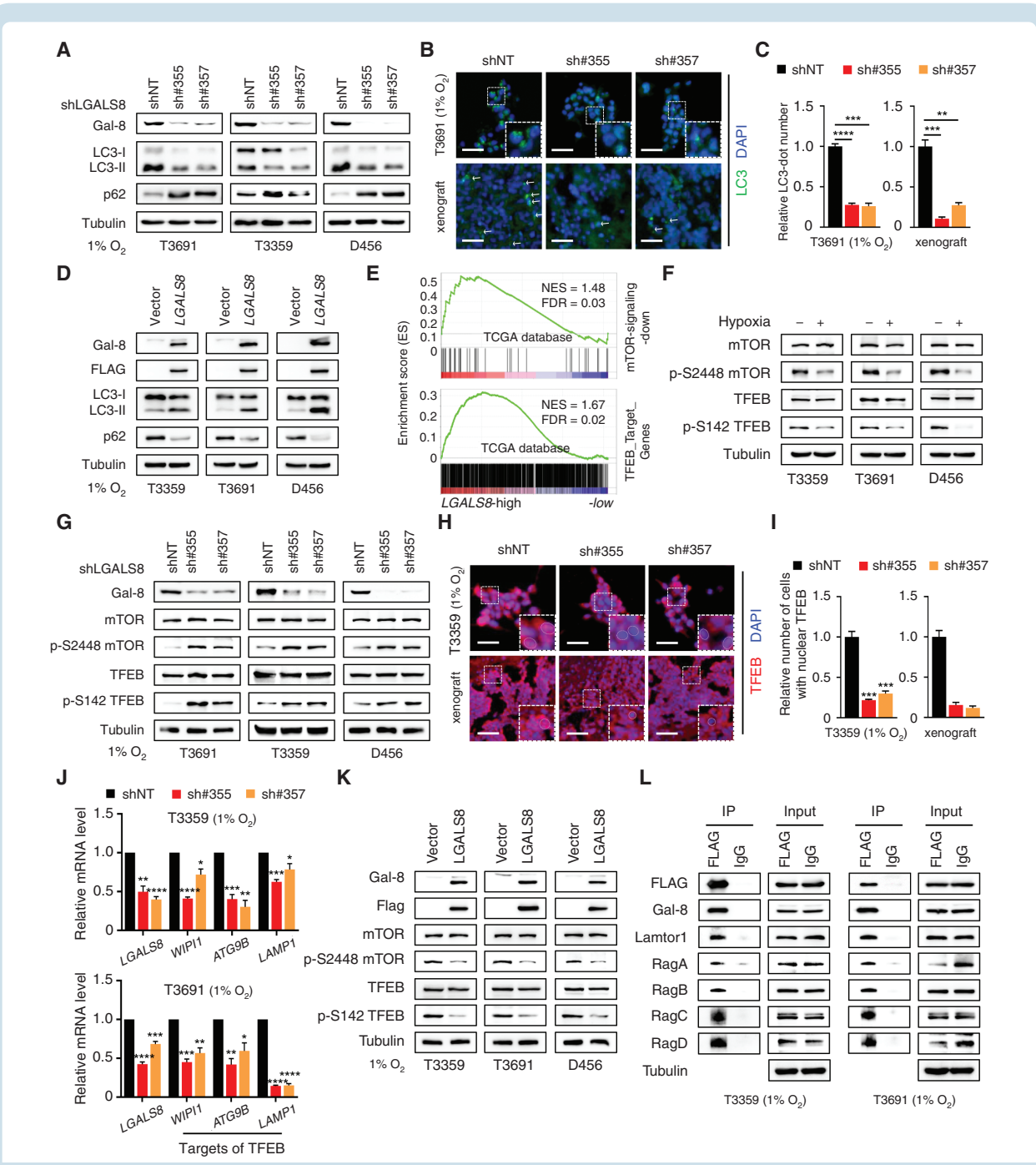

Figure 5. Gal-8 binds to the Ragulator-Rag complex to potentiate autophagy through the mTOR-TFEB axis. (A) Western blot analysis of Gal-8, LC3-I/II, and p62 expression in GSCs with Gal-8 knockdown under hypoxia. (B and C) IF staining of LC3 in GSCs with Gal-8 knockdown under hypoxia and xenografts derived from GSCs with Gal-8 knockdown (B). Quantification of relative LC3-dot number in each group (C). Blue: DAPI-labeled nuclei. Scale bar, 50 μm. (D) Western blot analysis of Gal-8, FLAG, LC3-I/II, and p62 expression in GSCs transduced with lentivirus expressing FLAG-*LGALS8* under hypoxia. (E) GSEA for mTOR-signaling-down and TFEB_Target_Genes signatures in LGALS8-high compared to LGALS8-low patients in the TCGA database. NES, normalized enrichment score; FDR, false discovery rate. (F) Western blot analysis of mTOR, p-S2448 mTOR, TFEB, p-S142 TFEB in GSCs cultured under normoxia or hypoxia for 24 h. (G) Western blot analysis of Gal-8, mTOR, p-S2448 mTOR, TFEB, and p-S142 TFEB expression in GSCs with Gal-8 knockdown under hypoxia. (H and I) IF staining of TFEB in GSCs with Gal-8 knockdown under hypoxia and xenografts derived from GSCs with Gal-8 knockdown (H). Quantification of relative nuclear TFEB in each group (I). Blue: DAPI-labeled nuclei. The dotted circles indicate outlines of the nucleus. Scale bar, 50 μm. (J) qRT-PCR analysis of Gal-8 and TFEB target genes (*WIP1*, *ATG9B*, *LAMP1*) expression in GSCs with Gal-8 knockdown under hypoxia. (K) Western blot analysis of Gal-8, mTOR, p-S2448 mTOR, TFEB, and p-S142 TFEB expression in GSCs transduced with lentivirus expressing FLAG-*LGALS8* under hypoxia. (L) Co-IP analysis in GSCs transduced with FLAG-*LGALS8* overexpression lentivirus. Cell lysates were immunoprecipitated with anti-FLAG antibodies followed by immunoblotting with anti-FLAG, anti-Gal-8, anti-Lamtor1, anti-RagA, anti-RagB, anti-RagC and anti-RagD antibodies. $^{*}P < .05$; $^{**}P < .01$; $^{***}P < .001$; $^{****}P < .0001$. Data are represented as mean ± SEM.

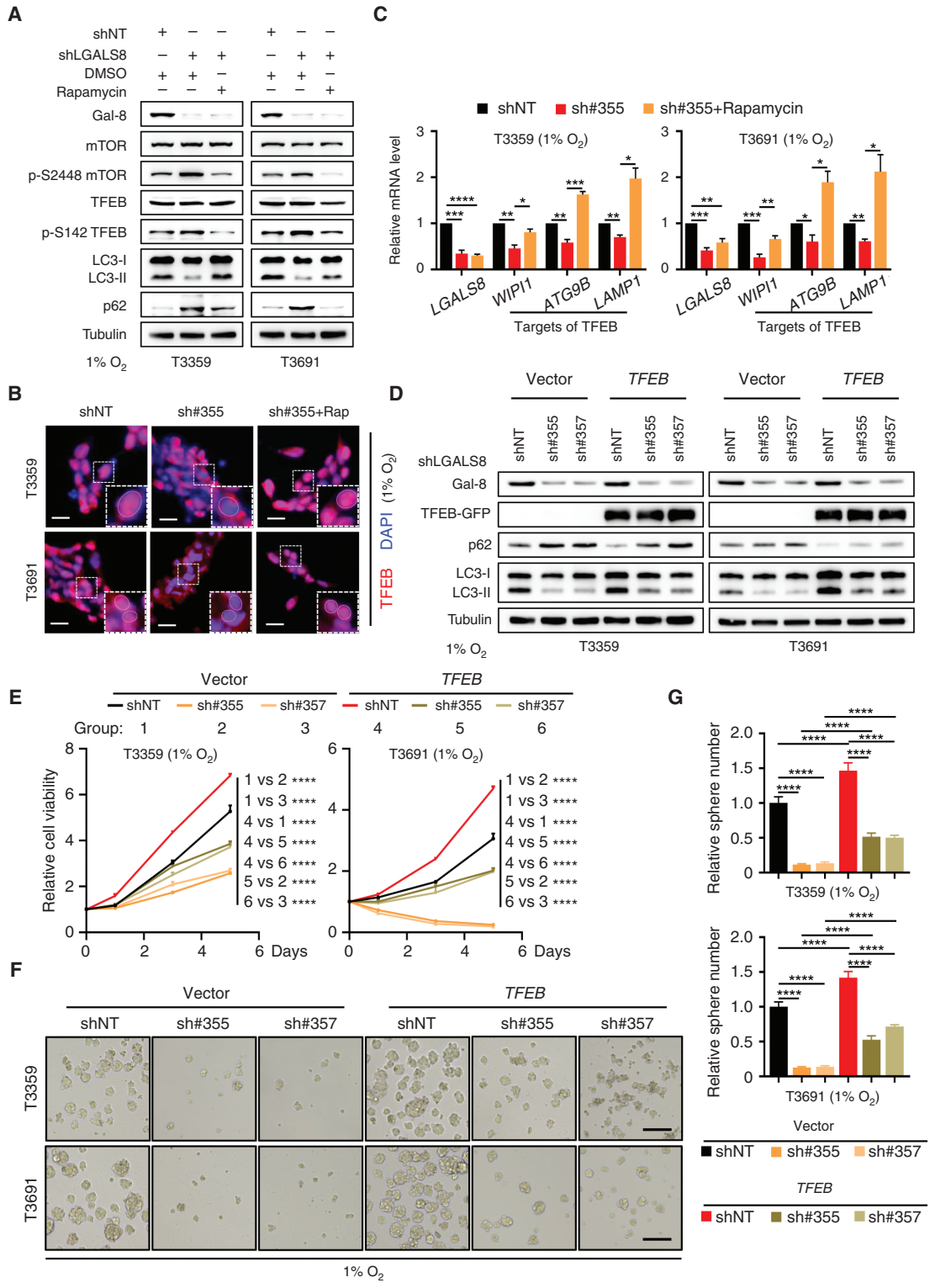

Figure 6. mTOR inhibition or TFEB overexpression mitigates the reduction in autophagy induced by Gal-8 depletion. (A) Western blot analysis of Gal-8, mTOR, p-S2448 mTOR, TFEB, p-S142 TFEB, LC3-I/II, and p62 expression in GSCs treated with Rapamycin following Gal-8 knockdown under hypoxia. (B) IF staining of TFEB in GSCs treated with Rapamycin following Gal-8 knockdown under hypoxia. Blue: DAPI-labeled nuclei. The dotted circles indicate outlines of the nucleus. Scale bar, 20 μm. (C) qRT-PCR analysis of Gal-8 and TFEB target genes (*WIP1*, *ATG9B*, *LAMP1*) expression in GSCs treated with Rapamycin after Gal-8 knockdown under hypoxia. (D) Western blots of Gal-8, TFEB-GFP, LC3-I/II, and p62 expression in GSCs with Gal-8 knockdown with/without TFEB overexpression under hypoxia. (E) Cell viability of GSCs with Gal-8 knockdown with/without lentivirus-mediated TFEB overexpression under hypoxia. (F and G) Sphereformation of GSCs with Gal-8 knockdown with/without lentivirus-mediated TFEB overexpression under hypoxia (F) and quantification of relative sphere number in each group (G). Scale bar, 100 μm. $^{*}P < .05$; $^{**}P < .01$; $^{***}P < .001$; $^{****}P < .0001$. Data are represented as mean ± SEM.

context-dependent role of autophagy in tumors, in addition to evidence that autophagy inhibition not only facilitates tumor progression but also suppresses tumor growth under varying conditions.[43] Therefore, to improve the efficacy of autophagy-targeted therapy, the regulatory functions of autophagy should be clarified concerning the cell type, microenvironment, and tumor types. Autophagy is found to be dysregulated in a variety of CSCs[44] and it has been shown to promote stemness maintenance, tumor growth, and resistance to treatment.[13,17,18,45] However, the majority of studies have been conducted under normoxia and the regulation of autophagy by hypoxia in GSCs has been scarcely investigated. Using pharmacological inhibitors and genetic approaches to manipulate autophagy, we have clearly shown that hypoxia enhances autophagy in GSCs, and autophagy inhibition is found to impair stemness maintenance in hypoxic GSCs. To the best of our knowledge, this study is the first to elucidate the regulation of autophagy regulation in GSCs by hypoxia. Moreover, using multiple screening methods, such as correlation and co-expression network analysis from various databases, we identify Gal-8 as an outstanding mediator of hypoxia-enhanced autophagy in GSCs and illustrate a mechanism by which Gal-8 regulated autophagy, specifically involving the mTOR-TFEB axis. Using multiple GSC lines in combination with the xenograft model, we have validated that the role of Gal-8 in autophagy is unique in GSCs as opposed to NSTCs, particularly, within hypoxic niches.

The transcription factor TFEB, a key modulator of autophagy and lysosomal biogenesis,[46] is regulated by mTOR in a phosphorylation-dependent manner.[26] Apart from its role in autophagy, TFEB also participates in the regulation of multiple fundamental cellular processes including lipid catabolism, energy metabolism, and immune response.[47] It is usually deregulated in various types of tumors and correlates with tumor progression.[47] TFEB was found to be overexpressed in GBM tissues in comparison to normal brains.[48] However, the expression and function of TFEB in GSC niches and hypoxic niches remain unknown. In this study, we verified that TFEB is activated to stimulate autophagy in GSCs under hypoxic conditions. This activation was attributed to the decreased phosphorylation of mTOR and TFEB, and overexpression of TFEB can counteract the mitigated autophagy caused by Gal-8 depletion, thereby preserving the stem cell characteristics.

In summary, our study reveals a hypoxic induction of the Gal-8-mTOR-TFEB axis that mediates the activation of autophagy and the maintenance of stemness in GSCs, by which GCSs sustain self-renewal during the progression of GBM.

Supplementary material

Supplementary material is available online at *Neuro-Oncology* (https://academic.oup.com/neuro-oncology).

Keywords

autophagy | galectin-8 | glioma stem cells | hypoxia |TFEB

Conflict of interest statement

The authors declare no competing interests.

Funding

This work was supported by grants from the National Natural Science Foundation of China (31900692, 32070961, 82072805), the National Key Research and Development Program of China (2023YFC251000), Hubei Provincial Natural Science Foundation of China (2020CFB678, 2023AFB135), Wuhan Science and Technology Major Project (2021022002023426) and the China Postdoctoral Science Foundation (2022M711253) and the postdoctoral innovation research position funding of Hubei province.

Acknowledgments

We thank Dr. Jeremy Rich and Dr. Shideng Bao for providing GSCs. ATG5 and AGT7 antibodies are kind gifts from Dr. Jianshuang Li. We thank Dr. Jiasheng Wu from the Department of Neurosurgery, Tongji Hospital, Tongji Medical College, Huazhong University of Science and Technology for his kind help on bioinformatic analysis. We thank Dr. Deonne Talyor for critically reading the manuscript.

Author contributions

D.L. and H.Z performed and analyzed the experiments. L.C., X.M., J.W. and Y.L. provided technical and scientific advice. R.L, J.W.W, S.J.Z, and K.S. provided the patient samples. D.L. and H.Z wrote the manuscript. K.S., X.Y., and C.L. conceptualized and designed the overall research and supervised the research.

Data Availability

All data generated or analyzed during this study are included in this published article and its supplementary information files.

Affiliations

Department of Medical Genetics, School of Basic Medicine, Tongji Medical College, Huazhong University of Science and Technology, Wuhan, China (D.L., Y.L., C.L.); Department of Neurosurgery, Tongji Hospital, Tongji Medical College, Huazhong University of Science and Technology, Wuhan, China (H.Z., L.C., R.L., X.M., J.W., J.W., S.Z., K.S.); Department of Histology and Embryology, School of Basic Medicine, Tongji Medical College, Huazhong University of Science and Technology, Wuhan, China (X.Y.)

References

1. Tan AC, Ashley DM, Lopez GY, et al. Management of glioblastoma: state of the art and future directions. *CA Cancer J Clin.* 2020;70(4):299–312.
2. Wen PY, Weller M, Lee EQ, et al. Glioblastoma in adults: a Society for Neuro-Oncology (SNO) and European Society of Neuro-Oncology (EANO) consensus review on current management and future directions. *Neuro-Oncol.* 2020;22(8):1073–1113.
3. Prager BC, Xie Q, Bao SD, Rich JN. Cancer stem cells: the architects of the tumor ecosystem. *Cell Stem Cell.* 2019;24(1):41–53.
4. Mitchell K, Troike K, Silver DJ, Lathia JD. The evolution of the cancer stem cell state in glioblastoma: emerging insights into the next generation of functional interactions. *Neuro-Oncol.* 2021;23(2):199–213.
5. Boyd NH, Tran AN, Bernstock JD, et al. Glioma stem cells and their roles within the hypoxic tumor microenvironment. *Theranostics.* 2021;11(2):665–683.
6. Guo XF, Qiu W, Liu QL, et al. Immunosuppressive effects of hypoxia-induced glioma exosomes through myeloid-derived suppressor cells via the miR-10a/Rora and miR-21/Pten pathways. *Oncogene.* 2018;37(31):4239–4259.
7. Yin J, Ge X, Shi Z, et al. Extracellular vesicles derived from hypoxic glioma stem-like cells confer temozolomide resistance on glioblastoma by delivering miR-30b-3p. *Theranostics.* 2021;11(4):1763–1779.
8. Wang P, Yan Q, Liao B, et al. The HIF1 alpha/HIF2 alpha-miR210-3p network regulates glioblastoma cell proliferation, dedifferentiation and chemoresistance through EGF under hypoxic conditions. *Cell Death Dis.* 2020;11(11):992.
9. Cowman SJ, Koh MY. Revisiting the HIF switch in the tumor and its immune microenvironment. *Trends Cancer.* 2022;8(1):28–42.
10. Qiang L, Wu T, Zhang HW, et al. HIF-1alpha is critical for hypoxia-mediated maintenance of glioblastoma stem cells by activating Notch signaling pathway. *Cell Death Differ.* 2012;19(2):284–294.
11. Man J, Yu X, Huang H, et al. Hypoxic induction of vasorin regulates notch1 turnover to maintain glioma stem-like cells. *Cell Stem Cell.* 2018;22(1):104–118.e6.
12. Klionsky DJ, Petroni G, Amaravadi RK, et al. Autophagy in major human diseases. *EMBO J.* 2021;40(19):e108863.
13. Hu CQ, Sun YT, Li WX, Bi Y. Hypoxia improves self-renew and migration of urine-derived stem cells by upregulating autophagy and mitochondrial function through ERK signal pathway. *Mitochondrion.* 2023;73:1–9.
14. El Hout M, Cosialls E, Mehrpour M, Hamai A. Crosstalk between autophagy and metabolic regulation of cancer stem cells. *Mol Cancer.* 2020;19(1):27.
15. Ulasov I, Fares J, Timashev P, Lesniak MS. Editing cytoprotective autophagy in glioma: An unfulfilled potential for therapy. *Trends Mol Med.* 2020;26(3):252–262.
16. Yan YL, Xu ZJ, Dai S, et al. Targeting autophagy to sensitive glioma to temozolomide treatment. *J Exp Clin Cancer Res.* 2016;35(1):23.
17. Huang TZ, Kim CK, Alvarez AA, et al. MST4 Phosphorylation of ATG4B regulates autophagic activity, tumorigenicity, and radioresistance in glioblastoma. *Cancer Cell.* 2017;32(6):840–855.e8.
18. Wang LH, Yuan Y, Wang J, et al. ASCL2 maintains stemness phenotype through ATG9B and sensitizes gliomas to autophagy inhibitor. *Adv Sci.* 2022;9(27):e2105938.
19. Tao Z, Li T, Ma H, et al. Autophagy suppresses self-renewal ability and tumorigenicity of glioma-initiating cells and promotes Notch1 degradation. *Cell Death Dis.* 2018;9(11):1063.
20. Zhu HT, Liu D, Cheng LD, et al. Prognostic value and biological function of galectins in malignant glioma. *Front Oncol.* 2022;12:834307.
21. Hu Y, Smyth GK. ELDA: extreme limiting dilution analysis for comparing depleted and enriched populations in stem cell and other assays. *J Immunol Methods.* 2009;347(1-2):70–78.
22. Bowman RL, Wang Q, Carro A, Verhaak RG, Squatrito M. GlioVis data portal for visualization and analysis of brain tumor expression datasets. *Neuro Oncol.* 2017;19(1):139–141.
23. Liu D, Zhu H, Li C. Galectins and galectin-mediated autophagy regulation: new insights into targeted cancer therapy. *Biomarker Res.* 2023;11(1):22.
24. Manero-Ruperez N, Martinez-Bosch N, Barranco LE, Visa L, Navarro P. The galectin family as molecular targets: hopes for defeating pancreatic cancer. *Cells.* 2020;9(3):689.
25. Bao SD, Wu QL, McLendon RE, et al. Glioma stem cells promote radioresistance by preferential activation of the DNA damage response. *Nature.* 2006;444(7120):756–760.
26. Napolitano G, Esposito A, Choi H, et al. mTOR-dependent phosphorylation controls TFEB nuclear export. *Nat Commun.* 2018;9(1):3312.
27. Saxton RA, Sabatini DM. mTOR signaling in growth, metabolism, and disease. *Cell.* 2017;168(6):960–976.
28. Jia JY, Abudu YP, Claude-Taupin A, et al. Galectins control mTOR in response to endomembrane damage. *Mol Cell.* 2018;70(1):120–135.e8.
29. Tribulatti MV, Carabelli J, Prato CA, Campetella O. Galectin-8 in the onset of the immune response and inflammation. *Glycobiology.* 2020;30(3):134–142.
30. Thurston TLM, Wandel MP, von Muhlinen N, Foeglein A, Randow F. Galectin 8 targets damaged vesicles for autophagy to defend cells against bacterial invasion. *Nature.* 2012;482(7385):414–418.
31. Beyer S, Wehrmann M, Meister S, et al. Galectin-8 and-9 as prognostic factors for cervical cancer. *Arch Gynecol Obstet.* 2022;306(4):1211–1220.
32. Ferragut F, Cagnoni AJ, Colombo LL, et al. Dual knockdown of galectin-8 and its glycosylated ligand, the activated leukocyte cell adhesion molecule (ALCAM/CD166), synergistically delays in vivo breast cancer growth. *Biochim Biophys Acta Mol Cell Res.* 2019;1866(8):1338–1352.
33. Labrie M, De Araujo LOF, Communal L, Mes-Masson AM, St-Pierre Y. Tissue and plasma levels of galectins in patients with high grade serous ovarian carcinoma as new predictive biomarkers. *Sci Rep.* 2017;7(1):13244.
34. Gentilini LD, Jaworski FM, Tiraboschi C, et al. Stable and high expression of galectin-8 tightly controls metastatic progression of prostate cancer. *Oncotarget.* 2017;8(27):44654–44668.
35. Chakraborty A, Perez M, Carroll JD, et al. Hypoxia controls the glycome signature and galectin-8-ligand axis to promote protumorigenic properties of metastatic melanoma. *J Invest Dermatol.* 2023;143(3):456–469.e8.
36. Gurung S, Fu H, Gu YH. The expression and clinical significance of galectin 8 in papillary thyroid cancer. *Int J Clin Exp Path.* 2016;9(7):6709–6723.
37. Liu YD, Xu L, Zhu Y, et al. Galectin-8 predicts postoperative recurrence of patients with localized T1 clear cell renal cell carcinoma. *Urol Oncol Semin Orig Investig.* 2015;33(3):112.e1–8.
38. Metz C, Doger R, Riquelme E, et al. Galectin-8 promotes migration and proliferation and prevents apoptosis in U87 glioblastoma cells. *Biol Res.* 2016;49(1):33.
39. Jing XM, Yang FM, Shao CC, et al. Role of hypoxia in cancer therapy by regulating the tumor microenvironment. *Mol Cancer.* 2019;18(1):157.
40. Rong Y, Durden DL, Van Meir EG, Brat DJ. 'Pseudopalisading' necrosis in glioblastoma: a familiar morphologic feature that links vascular pathology, hypoxia, and angiogenesis. *J Neuropathol Exp Neurol.* 2006;65(6):529–539.
41. Levy JMM, Towers CG, Thorburn A. Targeting autophagy in cancer. *Nat Rev Cancer.* 2017;17(9):528–542.
42. Rosenfeld MR, Ye X, Supko JG, et al. A phase I/II trial of hydroxychloroquine in conjunction with radiation therapy and concurrent and adjuvant temozolomide in patients with newly diagnosed glioblastoma multiforme. *Autophagy.* 2014;10(8):1359–1368.

43. Amaravadi RK, Kimmelman AC, Debnath J. Targeting autophagy in cancer: recent advances and future directions. *Cancer Discovery*. 2019;9(9):1167–1181.
44. Nazio F, Bordi M, Cianfanelli V, Locatelli F, Cecconi F. Autophagy and cancer stem cells: molecular mechanisms and therapeutic applications. *Cell Death Differ*. 2019;26(4):690–702.
45. Dolma S, Selvadurai HJ, Lan X, et al. Inhibition of dopamine receptor D4 impedes autophagic flux, proliferation, and survival of glioblastoma stem cells. *Cancer Cell*. 2016;29(6):859–873.
46. Tan A, Prasad R, Lee C, Jho EH. Past, present, and future perspectives of transcription factor EB (TFEB): mechanisms of regulation and association with disease. *Cell Death Differ*. 2022;29(8):1433–1449.
47. Napolitano G, Ballabio A. TFEB at a glance. *J Cell Sci*. 2016;129(13):2475–2481.
48. Giatromanolaki A, Sivridis E, Mitrakas A, et al. Autophagy and lysosomal related protein expression patterns in human glioblastoma. *Cancer Biol Ther*. 2014;15(11):1468–1478.